

## On the production of energetic neutrals in the cathode sheath of direct-current discharges

Tsuyohito Ito<sup>a)</sup> and Mark A. Cappelli

Mechanical Engineering Department, Stanford University, Stanford, California 94305-3032

(Received 29 November 2006; accepted 31 January 2007; published online 5 March 2007)

Direct measurements of the energy distribution of energetic neutrals incident onto the cathode of a dc glow discharge are presented. The measurements are performed by time-of-flight analysis of neutrals escaping through a cathode orifice. The experimental results are found to be in excellent agreement with Monte Carlo simulations, although the forward angle of the neutrals considered is limited in the present experimental configuration. It is found that the commonly used theories for the production of energetic neutrals through charge exchange in the cathode sheath do not capture the neutral energy distribution over the range of discharge voltage studied. © 2007 American Institute of Physics. [DOI: 10.1063/1.2711416]

Energetic neutrals formed by collisions with accelerated ions in the sheaths of direct-current (dc) discharges contribute to secondary electron emission, electrode erosion, and discharge gas heating. While many measurements have been made of the ion energy distribution in dc sheaths and a good agreement is seen with theoretical predictions,<sup>1–3</sup> with the exception of one preliminary indirect attempt,<sup>4</sup> there seems to be no direct measurements of the energy distribution of neutrals at the cathode in dc discharges. This is despite the availability of various theories<sup>5–8</sup> and computational studies.<sup>8–10</sup> The study of Ref. 4 employed an electron impact ionization source for filtering the energy of the original neutrals and detecting them as ions. The observed distributions are affected by this ionization process, in part due to the nonconstant probability of ionization, as pointed out by a study of the neutral energy distribution at the powered electrode of a rf argon discharge.<sup>11</sup> This letter presents direct time-of-flight (TOF) measurements of high energy neutrals impinging on the cathode in argon dc glow discharges. The variation in the energy distribution with discharge voltage is characterized and compared to theoretical predictions and Monte Carlo simulations. The results indicate that some theories<sup>5–7</sup> do not adequately describe neutral particle collisions in the cathode sheath and hence do not capture the neutral energy distribution for a broad range of discharge conditions.

The measurements were made of argon neutrals drifting parallel to the electric field direction, i.e., perpendicular to the cathode of a dc discharge cell, as shown in Fig. 1. The TOF apparatus is similar to that used to characterize energetic neutrals generated in fusion edge plasmas and from sputtering targets.<sup>12,13</sup> The abnormal dc glow discharges are generated in pure argon at a pressure of 0.5 Torr with a  $6 \times 10^{-2}$  m diameter copper cathode, a stainless-steel anode, and an electrode separation of  $5 \times 10^{-2}$  m. We have collected data for a range of values for the voltage and current, five combinations of which (350 V and  $1.4 \text{ A m}^{-2}$ , 390 V and  $2.0 \text{ A m}^{-2}$ , 460 V and  $4.8 \text{ A m}^{-2}$ , 540 V and  $8.3 \text{ A m}^{-2}$ , and 600 V and  $13 \text{ A m}^{-2}$ ) are selected for comparison to Monte Carlo (MC) simulations. Energetic neutrals formed near the

cathode by charge exchange collisions with impinging ions are sampled through a  $1 \times 10^{-4}$  m diameter orifice ( $\sim 5 \times 10^{-5}$  m thick cathode foil). The sampled beam is interrupted by a high-speed (20 000 rpm) chopper, placed  $3 \times 10^{-2}$  m downstream of the orifice, which contains a single  $3 \times 10^{-4}$  m wide slit ( $S_1$  in Fig. 1) on its blade,  $4 \times 10^{-2}$  m from the rotational axis. The drifting neutral stream impinges onto a 17 stage electron multiplier containing Cu–Be dynodes, located 0.9 m downstream of the chopper. A second ( $3 \times 10^{-3}$  m wide) slit ( $S_2$ ) is placed in front of the electron multiplier for improving temporal response. A positively biased grid [retarding grid (RG) in Fig. 1] is placed just downstream of the discharge cathode and the chopper to serve as an ion filter, allowing only neutrals to pass into the drift chamber and migrate towards the electron multiplier. It is verified that the threshold grid voltage required to filter out all of the ions is close to the discharge voltage, as expected. For the results described here, the ion filter voltage is set to at least 500 V higher than the discharge voltage. The solid angle collected by the spectrometer, as limited by the slit in front of the detector, is  $\sim 7.5 \times 10^{-5}$  sr. In comparing measurements to MC simulations, we consider the particles passing through the cathode orifice within this limited solid angle.

The drift chamber is pumped by two turbo molecular pumps maintaining a pressure of less than  $\sim 10^{-6}$  Torr during the measurements. At this pressure, the argon mean free path is longer than 50 m, so that the effects of collisions in the

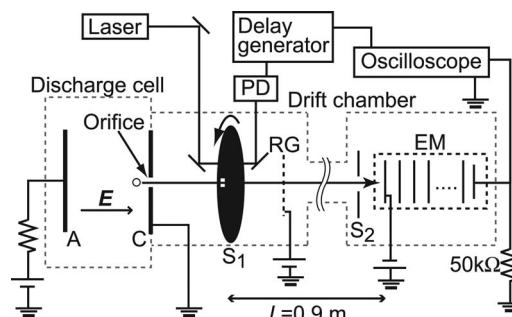


FIG. 1. Schematic of the experimental setup for measuring neutral energy distribution: anode (A), cathode (C), slits 1 and 2 ( $S_1$  and  $S_2$ ), positively biased ion RG, photo diode (PD), and electron multiplier (EM).

<sup>a)</sup>Present address: Graduate School of Engineering, Osaka University, 2-1 Yamadaoka, Suita, Osaka 565-0871, Japan.

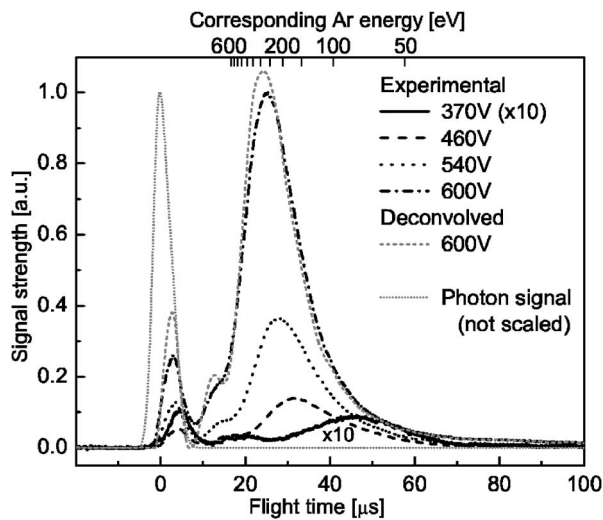


FIG. 2. Observed time-of-flight spectra for a range of discharge voltage, deconvolved spectrum for 600 V, and the photon signal used for the deconvolution process. TOF signals are normalized by the maximum value of the spectra for the 600 V discharge case.

drift chamber are negligible. A He–Ne laser modulated by the same chopper is used as a timing reference for triggering the oscilloscope, on which the TOF traces are recorded and averaged. The zero-drift time is determined by the signal corresponding to the detected photons from the discharge observed with reverse polarity (so that the orifice is now on the anode and there is little or no detected energetic neutral signal). The photon signal has a  $5 \mu\text{s}$  rise time with a full width at half maximum of  $5 \mu\text{s}$ , as shown in Fig. 2. This signal serves as an indication of the instrument broadening and is used to deconvolve the TOF spectra.

Representative experimental (uncorrected) TOF spectra for varying discharge voltage are shown in Fig. 2. The increases in signal intensity and a shift in peak position to shorter drift times with increasing voltage are apparent. The corresponding energy spectra are obtained following deconvolution and correction for the energy dependence of the secondary electron emission of neutral argon on Cu–Be.<sup>14</sup> It is noteworthy that the secondary electron emission can depend on surface conditions, as pointed out by Phelps and Petrović.<sup>15</sup> We have not pretreated or cleaned the Cu–Be dynode for these studies and therefore employ the secondary electron emission coefficient for untreated (native) Cu–Be surfaces, as reported in Ref. 14. The secondary electron emission also depends on energy, and the uncertainty in this energy dependence is the main source of error in the analysis. A compilation of the secondary electron emission of argon atoms incident on a range of untreated materials<sup>15</sup> shows that the coefficients (absolute and energy dependence) all fall within a factor of 2 of each other in the high energy region (e.g.,  $>100 \text{ eV}$ ). In this regime, we thus believe that the coefficients used in our study are accurate to within a factor of 2. In the low energy region ( $<100 \text{ eV}$ ), scatter in the data described in Ref. 15 precludes a certainty in the energy dependence of our extracted distributions to be better than a factor of  $\sim 3$ . Also shown in Fig. 2 are the photon signal and the 600 V case deconvolved for instrument broadening using this photon signal. As seen in the TOF spectra of Fig. 2, there are weak peaks between 0–5 and 10–20  $\mu\text{s}$ , the origin of which is attributed to hydrogen and oxygen contamination, perhaps as a result of sputtering of surfaces within the drift

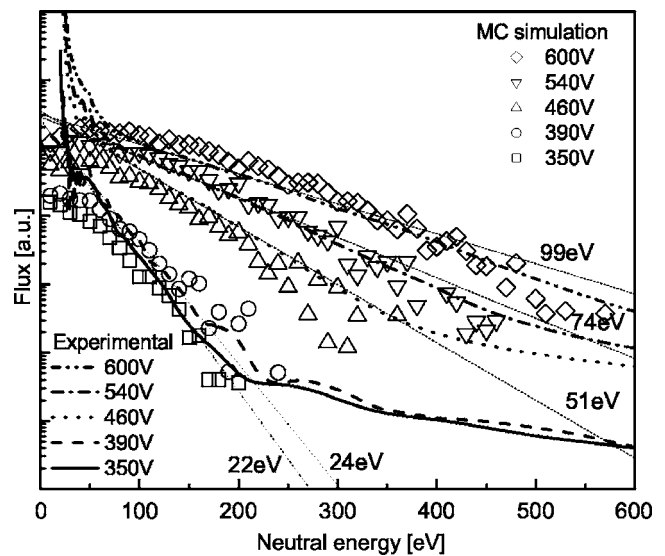


FIG. 3. Measured (thick lines) and MC simulations (symbols) of the neutral argon energy distribution. The thin dotted lines are superimposed Maxwellian distributions at the indicated temperatures, for comparison. Both the measured and simulated distributions are for neutral atoms sampled over the limited detection angle of the experiment.

section of the spectrometer. These peaks were not sensitive to Ar flow rate and there was only weak optical emission associated with hydrogen, and no emission due to oxygen, from the discharge itself, reducing the likelihood that this contamination originates in the discharge. These interferences precluded energy measurements beyond energies of approximately 200 eV for the lowest discharge voltage case shown (370 V) and about 500 eV for the highest discharge voltage shown (600 V). Operation of the discharge on helium confirmed that there is no contamination from heavier species that might overlap with the argon signal at lower energy.

Figure 3 shows the converted neutral energy spectra (thick lines). The variation in neutral energy distribution with discharge voltage is apparent, with a higher discharge voltage resulting in a more energetic high energy tail. The near-linear variation in the logarithmic energy distribution is indicative of an energetic tail that is close to Maxwellian. Thin dotted lines in the figure represent this Maxwellian tail at the labeled temperature. It is noteworthy, as mentioned above, that high energies might be affected by contamination from light elements such as H and O. The very low energy range (e.g.,  $<50 \text{ eV}$ ) is less accurate because of the low signal as a result of low secondary electron emission yields and because of the larger uncertainty in the secondary electron emission coefficient employed in the data reduction, as mentioned above.

The measurements are complimented by one-dimensional MC simulations, represented by the symbols in Fig. 3. The MC simulations use a sheath thickness and potential distribution determined from the collisional form of Child's law,<sup>16</sup> assuming a constant charge exchange cross section ( $Q_{\text{ch}}$ ) of  $4 \times 10^{-19} \text{ m}^2$ . In our MC simulations, particles collide in accordance with the energy-dependent collisional cross sections proposed by Phelps *et al.*<sup>17–19</sup> As seen from Fig. 3, good agreement is obtained between the measured neutral energy distributions and those predicted by the MC simulations. A closer comparison of the results of the

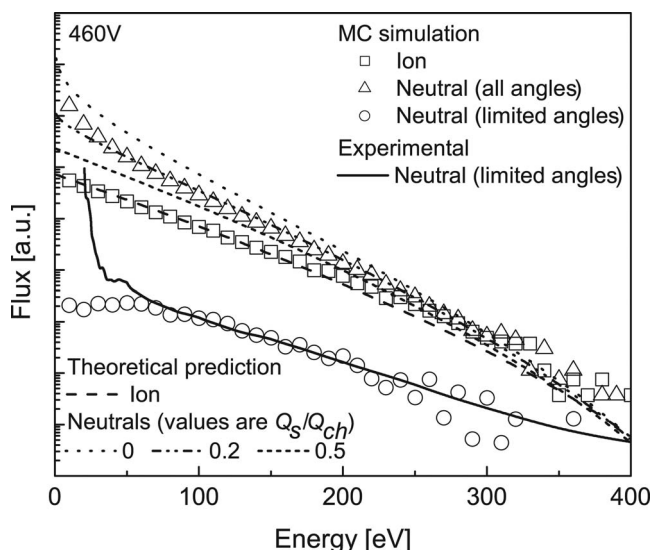


FIG. 4. Representative MC simulations and theoretical predictions (Refs. 1, 2, and 5–7) of ion and neutral energy distributions and the measured neutral energy distribution (0.5 Torr, 460 V, and  $4.8 \text{ A m}^{-2}$ ).

MC simulations, including the prediction of ion energy distributions, to the measurement and theory for the case of a 460 V discharge is provided in Fig. 4. Included in this figure are the MC predictions of neutral energy distributions considering all neutrals (labeled as “all angles”) and those neutrals that drift within the collection solid angle of the detector (labeled as “limited angles”). Again, we see that the agreement is quite good when limited angles are considered in the simulations, consistent with the limited solid angle collection of the experiment. Also shown in the figure are the theoretical predictions for the neutral energy distribution<sup>7</sup> based on an extension of the theory of Abril *et al.*<sup>5,6</sup> The values in the index are ratios of the so-called cross section for stopping neutrals by neutral-neutral collisions ( $Q_s$ ) to the cross section for ion-neutral charge exchange  $Q_{ch}$  ( $=4 \times 10^{-19} \text{ m}^2$ ).<sup>7</sup>  $Q_s$  represents the probability that a neutral collision occurs, resulting in a total loss of forward momentum. A value of zero for this ratio implies that all high energy neutrals created by charge exchange collisions arrive at the cathode without further energy loss, in accordance with the approach of Abril *et al.*<sup>5,6</sup> We see that a value of  $Q_s/Q_{ch}=0.2$  seems to lead to a similar distribution predicted by the MC simulations (considering all angles), even though this theory does not account for the scattering into shallow angles or energy exchange between neutrals by collisions. However, while this value provides agreement for the 460 V discharge case, a new value for this cross section ratio is found to be needed to obtain agreement at other discharge voltage conditions, i.e., there is no unique ratio of  $Q_s/Q_{ch}$  that captures the trends seen in all of the experiments, pointing to inadequacies in this simple theoretical description.<sup>5–7</sup> The theory by Hagelaar *et al.*<sup>8</sup>, which derived the highest and lowest limits for the neutral energy distributions through a rate equation based on a local field model, is not considered in this letter, since the use of a local field model may not be suitable for computing energy distributions in the cathode sheath (except perhaps for the very low energy portion of the ion energy distributions), where the electric field variation is significant. It is notewor-

thy that the ion velocities determined from the simulation are found to be nearly parallel to the electric field (with a peak at a small angle of  $\sim 3^\circ$ ) and the energy-dependent cross section used in the MC simulations results in good agreement with the ion energy distribution determined using the theory of Davis and Vanderslice<sup>1</sup> modified by Budtz-Jørgensen *et al.*<sup>2</sup>, as also shown in Fig. 4.

Revisiting Fig. 3, we draw attention to the MC simulations of the neutral energy distribution (for neutrals scattered over limited angles) and their comparison to the measured distributions for the same limited angles. The agreement between experiments and MC simulations (which have, as an input, the experimental discharge current and voltage) is remarkable. In particular, it is noteworthy that the relative intensity with varying voltage for either the predicted or measured distributions is not adjusted once the experimental distribution for the 350 V case is scaled to overlap with that simulated.

To summarize, this letter represents the first direct measurement of the energy distribution of neutral particles incident onto the cathode of a dc glow discharge. The measurements are in good agreement with MC simulations, although in both cases, the forward angle of the neutrals considered or sampled in the experiments is limited to the corresponding solid angle of detection by the TOF spectrometer. While simple theories using constant cross sections for charge exchange and forward momentum loss collisions provide some agreement with experiments over a limited range of conditions, these theories do not provide agreement over a broad range of conditions. Further refinements in the MC simulations would involve consideration of the differential cross section for ion-neutral scattering collisions.

The authors would like to thank W. S. Crawford for technical support. This research was funded in part by the NSF and DOE. Support for one of the authors (T.I.) was provided by the JSPS Postdoctoral Fellowships for Research Abroad program.

<sup>1</sup>W. D. Davis and T. A. Vanderslice, *Phys. Rev.* **131**, 219 (1963).

<sup>2</sup>C. V. Budtz-Jørgensen, J. Bøttiger, and P. Kringhøj, *Vacuum* **56**, 9 (2003).

<sup>3</sup>T. Ito and M. A. Cappelli, *Phys. Rev. E* **73**, 046401 (2006).

<sup>4</sup>D. G. Armour, H. Valisadeh, F. A. H. Soliman, and G. Carter, *Vacuum* **34**, 295 (1984).

<sup>5</sup>I. Abril, A. Gras-Marti, and J. A. Vallés-Abarca, *Phys. Rev. A* **28**, 3677 (1983).

<sup>6</sup>I. Abril, A. Gras-Marti, and J. A. Vallés-Abarca, *J. Phys. D* **17**, 1841 (1984).

<sup>7</sup>R. S. Mason and R. M. Allott, *J. Phys. D* **27**, 2372 (1994).

<sup>8</sup>G. J. M. Hagelaar, G. M. W. Kroesen, and M. H. Klein, *J. Appl. Phys.* **88**, 2240 (2000).

<sup>9</sup>V. V. Serikov and K. Nanbu, *J. Appl. Phys.* **82**, 5948 (1997).

<sup>10</sup>I. Revel, L. C. Pitchford, and J. P. Boeuf, *J. Appl. Phys.* **88**, 2234 (2000).

<sup>11</sup>J. Janes and K. Börnig, *J. Appl. Phys.* **73**, 2724 (1993).

<sup>12</sup>D. E. Voss and S. A. Cohen, *Rev. Sci. Instrum.* **53**, 1696 (1982).

<sup>13</sup>K. Tominaga, M. Kume, T. Yuasa, and O. Tada, *Jpn. J. Appl. Phys., Part 1* **24**, 35 (1985).

<sup>14</sup>K. Kadota and Y. Kaneko, *Jpn. J. Appl. Phys.* **13**, 1554 (1974).

<sup>15</sup>A. V. Phelps and Z. Lj. Petrović, *Plasma Sources Sci. Technol.* **8**, R21 (1999).

<sup>16</sup>M. A. Lieberman and A. J. Lichtenberg, *Principles of Plasma Discharges and Materials Processing* (Wiley, New York, 1994), p. 170.

<sup>17</sup>A. V. Phelps, *J. Appl. Phys.* **76**, 747 (1994).

<sup>18</sup>A. V. Phelps (private communication); <http://jilawww.cololado.edu/~avp/>

<sup>19</sup>A. V. Phelps, C. H. Green, and J. P. Burke, Jr., *J. Phys. B* **33**, 2965 (2000).